INTERNATIONAL JOURNAL OF ADAPTIVE CONTROL AND SIGNAL PROCESSING
Int. J. Adapt. Control Signal Process. 2009; **0**:1–21 *Prepared using* acsauth.cls *[Version: 2002/11/11 v1.00]*

3D Navigation and Collision Avoidance for nonholonomic aircraft-like vehicles

Giannis Roussos[1,*,†], Dimos V. Dimarogonas[2,‡] and Kostas J. Kyriakopoulos[1,§]

[1] *Control Systems Lab, Department of Mechanical Engineering, National Technical University of Athens, 9 Heroon Polytechniou Street, Zografou 15780, Greece.*
[2] *Laboratory for Information and Decision Systems, Massachusetts Institute of Technology, 77 Massachusetts Avenue, Cambridge, MA 02139-4307, USA*

SUMMARY

This paper extends the Navigation Function methodology to the case of 3D nonholonomic vehicles, both in single agent and multi-agent problems. The kinematic, nonholonomic, 3-dimensional model considered is chosen to resemble the motion of an aircraft by preventing any movement along the lateral or perpendicular axis, as well as preventing high yaw rotation rates. The discontinuous feedback control law used is based on the artificial potential field generated by Dipolar Navigation Functions and steers the agents away from obstacles or each other and towards their destinations, while respecting the nonholonomic constraints present. The convergence properties of the proposed control strategies are formally guaranteed and verified by non-trivial simulation results.

KEY WORDS: collision avoidance, air traffic control, nonholonomic control, multi-agent systems

1. INTRODUCTION

nonholonomic systems [1] are of great interest in the control community since they apply to a number of real world paradigms, e.g. wheeled mobile robots, Autonomous Underwater Vehicles (AUVs) and Unmanned Aerial Vehicles (UAVs), or automated Air Traffic Control (ATM) in general. In such applications stabilisation to a goal configuration, along with collision avoidance with static obstacles or other agents operating in the same area, is required.

It was shown in [2] that nonholonomic systems cannot be stabilised by any time invariant, smooth state feedback controller, requiring either a time varying or a discontinuous controller. Astolfi [3], Canudas de Wit et. al. [4] and Bloch et. al. [5] have proposed control schemes for the stabilisation of a single nonholonomic vehicle using a discontinuous control law, although no collision avoidance strategy has been incorporated. Approaches that additionally perform obstacle avoidance using

*Correspondence to: Giannis Roussos, Control Systems Lab, Department of Mechanical Engineering, National Technical University of Athens, 9 Heroon Polytechniou Street, Zografou 15780, Greece.
†email: jrous@mail.ntua.gr
‡email: ddimar@mit.edu
§email: kkyria@mail.ntua.gr

Navigation Functions [6] have been proposed by Lopes and Koditschek [7] and Tanner et. al. [8]. Decentralized control for multi-agent systems using Navigation Functions has also been presented [9]. The aforementioned approaches address 2-dimensional problems, like ground vehicles or aircraft flying on a constant altitude level. For applications that are inherently 3-dimensional, like aircraft flying in 3-dimensional space or underwater vehicles, the above solutions cannot be directly applied since the extension to 3-dimensional problems is not trivial. An augmented model of motion is required in 3D problems, which will comply with the kinematic constraints present in the real system.

Previous work on the control of 3D nonholonomic agents include approaches by Aicardi et al. based on a velocity vector field [10], [11] and tracking of a 2D path that has been expanded empirically to 3D space [12]. It should be noted though that in these approaches no obstacle avoidance method is used, while the bank angle of the vehicle is not controlled. An approach including obstacle avoidance for a single agent has been proposed by the authors in [13]. . Formulating collision avoidance as an optimisation problem [14], [15], [16] can yield efficient solutions. However, large computational resources are usually required is such approaches, making optimisation more relevant to centralised implementations and long-term collision avoidance. The work presented here is aimed mostly at short-term collision avoidance, where safety considerations are more important than efficiency and optimality.

This paper presents a novel method for the independent control of multiple 3-dimensional spherical agents using a kinematic controller in combination with *Dipolar Navigation Functions* [8]. The nonholonomic model used for the agents is chosen to represent aircraft flying in 3-dimensional space, as it takes into account the kinematic constraints on the lateral and perpendicular motion that apply on an aircraft. Furthermore, the control law is more intuitive and less conservative than previous Navigation Function based controllers [9], while being engineered to keep the yaw rotation rate to a minimum [13], as is common for a conventional fixed-wing aircraft. This control strategy forces the agents to follow feasible nonholonomic trajectories that avoid collisions with each other or the workspace boundary and lead to the desired configuration. Being a reactive method, this approach is robust with respect to modeling or measurement errors.

The applicability of our approach to ATM is discussed and necessary conditions are given, resulting in reasonable requirements. The work presented here is motivated by the envisioned decentralisation of ATM in the future. This will be needed to handle the increased traffic density of the next decades. Our algorithm uses real-time sensing in a reactive manner to guide the aircraft. This will be supported by future information exchange and processing systems that will be included in aircraft's equipment.

The rest of the paper is organized as follows: Section 2 describes the nonholonomic model used for the agents, Section 3 presents the control scheme for the single agent case with stationary obstacles while in the next Section the control strategy for the multi-agent problem is given. Section 5 presents simulation results for both cases that demonstrate the effectiveness of the methodology, while the conclusions of the paper are summarized in Section 6.

2. MODEL OF AGENTS

We consider 1 or N kinematic nonholonomic agents evolving in three dimensional space. The state $\mathbf{n}_i$ of each agent i, $i = 1, ..., N$ consists of its position $\mathbf{n}_{i1}$ and orientation $\mathbf{n}_{i2}$ [17]:

$$\mathbf{n}_i = \begin{bmatrix} \mathbf{n}_{i1} \\ \mathbf{n}_{i2} \end{bmatrix}, \quad \mathbf{n}_{i1} = \begin{bmatrix} x_i \\ y_i \\ z_i \end{bmatrix}, \quad \mathbf{n}_{i2} = \begin{bmatrix} \phi_{i1} \\ \phi_{i2} \\ \phi_{i3} \end{bmatrix}$$

where $\left[\begin{array}{ccc}\phi_{i1} & \phi_{i2} & \phi_{i3}\end{array}\right]^\top$ are xyz Euler angles. Let this *Earth-fixed* coordinate system follow the *NED* (*North-East-Down*) convention with x_i pointing North, y_i East, and z_i Down. Consequently $\phi_{i1},\ \phi_{i2},\ \phi_{i3}$ express *bank*, *elevation* and *azimuth* angles respectively, as shown in Figure 1. In order to avoid ambiguity in the orientation representation we enforce the normalization of angles to the following limits: $\phi_{i1} \in (-\pi, \pi]$, $\phi_{i2} \in \left(-\frac{\pi}{2}, \frac{\pi}{2}\right]$, $\phi_{i3} \in (-\pi, \pi]$. The motion of agent i is described by:

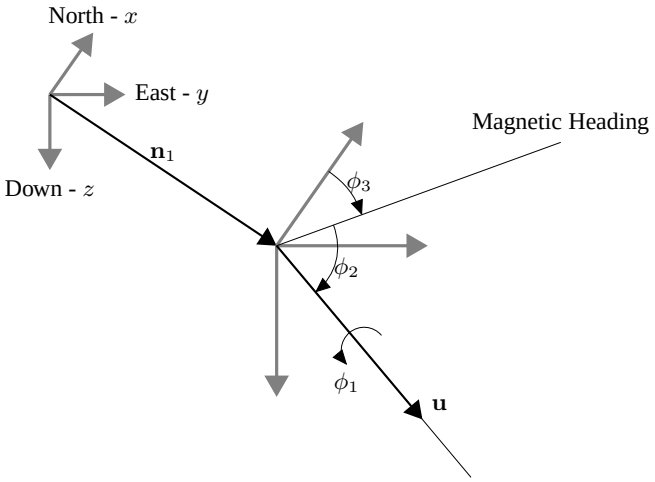

Figure 1: Earth Fixed Coordinates

$$\dot{\mathbf{n}}_i = \boldsymbol{\tau}_i = \left[\begin{array}{c}\boldsymbol{\tau}_{i1}\\ \boldsymbol{\tau}_{i2}\end{array}\right] = \left[\begin{array}{c}\dot{\mathbf{n}}_{i1}\\ \dot{\mathbf{n}}_{i2}\end{array}\right]$$

where $\boldsymbol{\tau}_{i1} = \left[\begin{array}{c}s_{i1}\\ s_{i2}\\ s_{i3}\end{array}\right]$ and $\boldsymbol{\tau}_{i2} = \left[\begin{array}{c}\omega_{i1}\\ \omega_{i2}\\ \omega_{i3}\end{array}\right]$ are the linear and angular velocities respectively.

As stated above the type of agent under consideration is nonholonomic, resembling an aircraft, i.e., there are nonholonomic constraints expressed in the *Body-Fixed* coordinate system which is described below (the index i has been omitted for the rest of this section for notational efficiency):

1. *Position and Orientation in the Body-Fixed System*

$$\mathbf{r} = \left[\begin{array}{c}\mathbf{l}\\ \mathbf{a}\end{array}\right], \quad \mathbf{l} = \left[\begin{array}{c}l_1\\ l_2\\ l_3\end{array}\right], \quad \mathbf{a} = \left[\begin{array}{c}a_1\\ a_2\\ a_3\end{array}\right]$$

   where $\mathbf{l}$ is the position and $\mathbf{a}$ the orientation (in xyz Euler angles), expressed in the body fixed coordinates. l_1 points forward, l_2 to the right and l_3 downwards with respect to the agent.
2. *Body-Fixed Linear and Angular Velocities*

$$\mathbf{v} = \left[\begin{array}{c}\mathbf{v}_1\\ \mathbf{v}_2\end{array}\right], \quad \mathbf{v}_1 = \left[\begin{array}{c}u\\ v\\ w\end{array}\right], \quad \mathbf{v}_2 = \left[\begin{array}{c}p\\ q\\ r\end{array}\right]$$

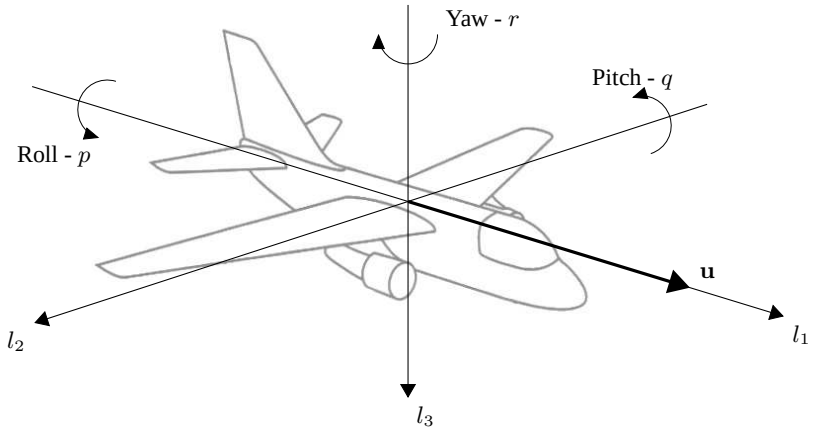

Figure 2: Body-Fixed Coordinates

u, v, w are the linear velocities along the body fixed axes, while p, q, r are the body-fixed *roll*, *pitch* and *yaw* rotation rates respectively, as shown in Figure 2.

The transformation between body-fixed and earth-fixed velocities is described in [17]:

$$\dot{\mathbf{n}}_1 = \boldsymbol{\tau}_1 = \mathbf{J}_1(\mathbf{n}_2) \cdot \mathbf{v}_1 \tag{1a}$$

$$\dot{\mathbf{n}}_2 = \boldsymbol{\tau}_2 = \mathbf{J}_2(\mathbf{n}_2) \cdot \mathbf{v}_2 \tag{1b}$$

$$\text{where} \quad \mathbf{J}_1 = \begin{bmatrix} c\phi_3 c\phi_2 & -s\phi_3 c\phi_1 + c\phi_3 s\phi_2 s\phi_1 & s\phi_3 s\phi_1 + c\phi_3 c\phi_1 s\phi_2 \\ s\phi_3 c\phi_2 & c\phi_3 c\phi_1 + s\phi_1 s\phi_2 s\phi_3 & -c\phi_3 s\phi_1 + s\phi_2 s\phi_3 c\phi_1 \\ -s\phi_2 & c\phi_2 s\phi_1 & c\phi_2 c\phi_1 \end{bmatrix} \in SO(3),$$

$$\mathbf{J}_2 = \begin{bmatrix} 1 & s\phi_1 t\phi_2 & c\phi_1 t\phi_2 \\ 0 & c\phi_1 & -s\phi_1 \\ 0 & \frac{s\phi_1}{c\phi_2} & \frac{c\phi_1}{c\phi_2} \end{bmatrix}$$

using the notation $s\cdot = \sin(\cdot),\ c\cdot = \cos(\cdot),\ t\cdot = \tan(\cdot)$.

The input vector of the *kinematic* nonholonomic system under consideration is

$$\mathbf{v}_K = \begin{bmatrix} u & \omega_1 & \omega_2 & \omega_3 \end{bmatrix}^\top$$

i.e. only the longitudinal (body-fixed) linear velocity u and the three earth-fixed rotation rates $\omega_1, \omega_2, \omega_3$ are actuated, while $v = w = 0$. Such a model resembles better the motion of an aircraft as it does not allow any motion along the body-fixed lateral l_2 or perpendicular l_3 axis. Given that according to the selected input vector $v = w = 0$, the 2^{nd} and 3^{rd} column of $\mathbf{J}_1(\mathbf{n_2})$ can be omitted to derive the complete agent model considered in this paper:

$$\dot{\mathbf{n}} = \tau = \begin{bmatrix} \boldsymbol{\tau}_1 \\ \boldsymbol{\tau}_2 \end{bmatrix} = \mathbf{R}(\mathbf{n}_2) \cdot \mathbf{v}_K \tag{2}$$

$$\text{where } \mathbf{R} = \begin{bmatrix} \mathbf{J}_I & \mathbf{0}_{3\times 3} \\ \mathbf{0}_{3\times 1} & \mathbf{I}_3 \end{bmatrix} \in \mathbb{R}^{6\times 4},\ \mathbf{J}_I = \mathbf{J}_I(\mathbf{n}_2) = \begin{bmatrix} c\phi_3 c\phi_2 \\ s\phi_3 c\phi_2 \\ -s\phi_2 \end{bmatrix}$$

3. 3D NAVIGATION FOR A SINGLE AGENT WITH OBSTACLE AVOIDANCE

3.1. Problem Statement

The problem under consideration in this section is to design a control law that will steer a single agent described by (2) to a desired position and orientation, $\mathbf{n}_{1d}$ and $\mathbf{n}_{2d} = \begin{bmatrix} \phi_{1d} & \phi_{2d} & \phi_{3d} \end{bmatrix}^\top$ respectively, while avoiding collisions with any of the m_0 stationary spherical obstacles of radii $r_{Oi}, \quad i = 1, \ldots, m_O$, located in positions $\mathbf{n}_{Oi}$ inside the workspace $W \subset \mathbb{R}^3$, or the workspace's boundary ∂W. Spherical agent and workspace are assumed, with radii r and r_{world} respectively.

3.2. Dipolar Navigation Function in 3D Space

Navigation Functions are not suitable for the control of a nonholonomic agent, as they do not take into account the kinematic constraints that apply on such a vehicle. Use of the original Navigation Function as introduced by Koditschek and Rimon in [6] with a feedback law for the control of a nonholonomic agent can lead to undesired behavior, like having the agent rotate in place. In order to overcome this difficulty *Dipolar Navigation Functions* have been developed [8], that offer a significant advantage: the integral lines of the resulting potential field are all tangent to the desired orientation at the destination. This property eliminates the need for in-place rotation, as the agent is driven to the destination with the desired orientation. This is achieved by considering the plane of which the normal vector is parallel to the desired orientation, and includes the destination, as an additional artificial obstacle.

The Navigation Function used in this paper is an extension of previous 2D approaches to the 3D case considered here:

$$\Phi = \frac{\gamma_d}{\left(\gamma_d^k + H_{nh} \cdot G \cdot \beta_0\right)^{1/k}} \tag{3}$$

where: $\gamma_d = ||\mathbf{n}_1 - \mathbf{n}_{1d}||^2$ is the distance from the destination position $\mathbf{n}_{1d}$,

$$G = \prod_{i=1}^{m_O} g_i, \quad \text{a measure of the proximity to obstacles}$$

$$g_i = ||\mathbf{n}_1 - \mathbf{n}_{Oi}||^2 - (r + r_{Oi})^2,$$

$$\beta_0 = r_{world}^2 - ||\mathbf{n}_1||^2 - r^2, \quad \text{the workspacing bounding obstacle}$$

The factor H_{nh} renders the potential field dipolar. It creates the repulsive potential of the artificial obstacle, used to align the trajectories at the destination with the desired orientation $\mathbf{n}_{2d}$:

$$\begin{aligned} H_{nh} &= \epsilon_{nh} + n_{nh} \\ n_{nh} &= \left|\left|\mathbf{J}_{Id}^\top \cdot (\mathbf{n}_1 - \mathbf{n}_{1d})\right|\right|^2 \\ \mathbf{J}_{Id} &= \mathbf{J}_I\left(\mathbf{n}_{2d}\right) \end{aligned}$$

where ϵ_{nh} is a small positive constant. Finally, k is a positive tuning parameter for this class of Navigation Functions.

The potential field created by a Dipolar Navigation Function (3), as the one shown in Figure 3, has guaranteed navigation properties, i.e. it provides almost global convergence to the destination along with guaranteed collision avoidance. The term 'almost' is used here because as Rimon et. al. [6] have

shown, there is a minimum of one saddle point in the potential field per obstacle in the workspace. Moreover, there is a set of initial conditions that lead the system to each saddle point. This is not important practically though, as these sets have zero measure and such initial conditions are extremely rare, even in simulations. Therefore, as is common in Navigation Function based approaches, in the rest of this paper we assume that the initial conditions lie outside of those sets, and no saddle points can ever be reached.

The potential of such a Navigation Function in a 2D workspace with 2 obstacles O_1, O_2 is shown in Figure 3. The target is $\begin{bmatrix} x_d & y_d \end{bmatrix} = \begin{bmatrix} 7 & 0 \end{bmatrix}$, with orientation $\phi_d = 0$ and the corresponding nonholonomic obstacle H is the line $x = 7$.

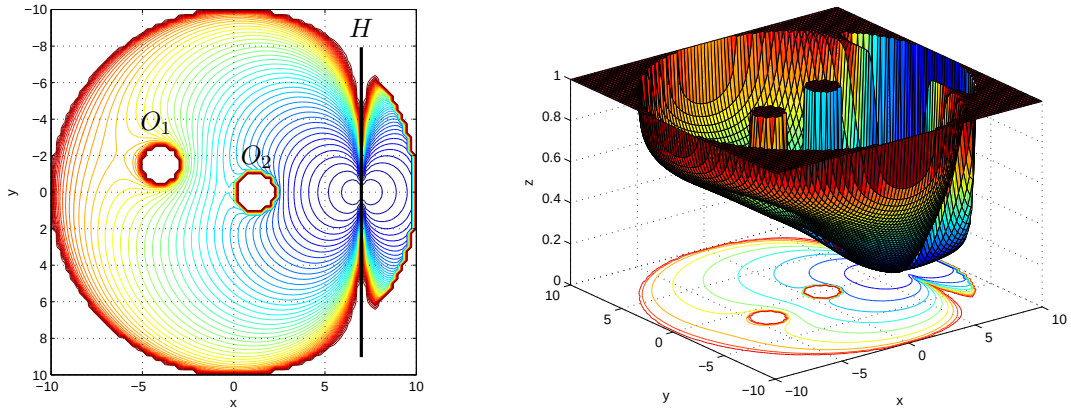

Figure 3: Potential of a Navigation Function in a 2D workspace with 2 obstacles O_1, O_2. The target is with orientation $\phi_d = 0$ and the corresponding nonholonomic obstacle H is the line $x = 7$.

3.3. Control Law

The proposed kinematic control law is based on the one proposed in [8], adapted to the 3-dimensional case:

$$u = -\operatorname{sgn}(\mathbf{J}_I^{\top} \frac{\partial \Phi}{\partial \mathbf{n}_1}) \cdot F(\mathbf{n}_1) \tag{4a}$$

$$\omega_k = -k_{\phi_k} (\phi_k - \phi_{\mathbf{nh}k}), \quad k = 1, 2, 3 \tag{4b}$$

where the function $F = k_u \cdot \left|\left| \frac{\partial \Phi}{\partial \mathbf{n}_1} \right|\right|^2 + k_z \cdot ||\mathbf{n}_1||^2$ regulates the magnitude of the linear velocity, $\Phi = \Phi(n_1)$ is the above *Dipolar Navigation Function* (3), k_u, k_z, k_{ϕ_k} are positive real gains and the function sgn is:

$$\operatorname{sgn}(x) \triangleq \begin{cases} 1, & \text{if } x \geq 0 \\ -1, & \text{if } x < 0 \end{cases}$$

Let function $\operatorname{atan2}$ be defined by:

$$\operatorname{atan2}(y, x) \triangleq arg\,(x, y), \quad (x, y) \in \mathbb{C}$$

The *nonholonomic angles* $\phi_{\mathbf{nh}k}$, $k = 1, 2, 3$ are determined by the components of the gradient vector $\mathrm{sgn}(x)\nabla\Phi$:

$$\phi_{\mathbf{nh}3} \triangleq \mathrm{atan2}\left(\mathrm{sgn}(x)\Phi_y, \mathrm{sgn}(x)\Phi_x\right) \tag{5a}$$

$$\phi_{\mathbf{nh}2} \triangleq \mathrm{atan2}\left(-\mathrm{sgn}(x)\Phi_z, \sqrt{{\Phi_x}^2 + {\Phi_y}^2}\right) \tag{5b}$$

$$\phi_{\mathbf{nh}1} \triangleq \mathrm{atan2}\left(\mathrm{sgn}(x)\, c\phi_2 \cdot \omega_3, \mathrm{sgn}(x)\, \omega_2\right) \tag{5c}$$

where $\Phi_x = \frac{\partial\Phi}{\partial x}$, $\Phi_y = \frac{\partial\Phi}{\partial y}$, $\Phi_z = \frac{\partial\Phi}{\partial z}$. The angles $\phi_{\mathbf{nh}2}$ and $\phi_{\mathbf{nh}3}$ represent the direction (azimuth and elevation) of the vector $\mathrm{sgn}(x)\nabla\Phi$ [18], which is the direction that the longtitudal axis l_1 steers to align with. When $x < 0$ the agent must approach the target moving forward so it steers towards the direction of $-\nabla\Phi$, while when $x > 0$ the control law steers the agent to the direction of $\nabla\Phi$ in order to approach the target moving backwards.

Because the above defined angles are discontinuous at the destination $\mathbf{n}_{1d}$ (where the gradient vector is zero) we employ an approximation scheme [19]:

$$\hat{\phi}_{\mathbf{nh}k} \triangleq \begin{cases} \phi_{\mathbf{nh}k}, & \rho_k > \epsilon \\ \dfrac{\phi_{\mathbf{nh}k}\left(-2\rho_k^3 + 3\epsilon\rho_k^2\right) + \phi_{kd}\left(-2\left(\epsilon - \rho_k\right)^3 + 3\epsilon\left(\epsilon - \rho_k\right)^2\right)}{\epsilon^3}, & \rho_k \leq \epsilon \end{cases}$$

for $k = 1, 2, 3$, where $\rho_1 = \sqrt{c\phi_2^2 \cdot \omega_3^2 + \omega_2^2}$, $\rho_2 = ||\nabla_i \Phi_i||$ and $\rho_3 = \sqrt{\Phi_{ix}^2 + \Phi_{iy}^2}$. Thus, the angles $\hat{\phi}_{\mathbf{nh}k}$ are continuous when $\rho_k = 0$ as $\lim_{\rho_k \to 0} \hat{\phi}_{\mathbf{nh}k} = \hat{\phi}_{\mathbf{nh}k}\Big|_{\rho_k = 0} = \phi_{kd},\ k = 1, 2, 3$. Therefore at the destination we have:

$$\hat{\phi}_{\mathbf{nh}k}\Big|_{\mathbf{n}_1 = \mathbf{n}_{1d}} = \phi_{kd},\ k = 1, 2, 3 \tag{6}$$

The control law for the longtitudal velocity drives the agent either forward or backwards, depending on the sign of the projection of $\frac{\partial\Phi}{\partial \mathbf{n}_1}$ on the body-fixed longtitudal l_1 axis, so that the navigation function is decreasing along the direction of movement.

The bank angle control law (ω_1) is designed to track the reference bank angle $\phi_{\mathbf{nh}1}$, so that the agent tends to eliminate the yaw rate r and achieve the required alignment only through pitch rotation q, as is natural for an aircraft. In other words, the body-fixed l_3 axis is driven to align with the curvature vector $\nabla^2\Phi$ of the trajectory defined by the Navigation Function. In fact it can be easily shown that the desired bank angle $\phi_{\mathbf{nh}1}$, as defined above, eliminates the yaw rate in the body-fixed coordinate system. To do this, we can use the inverse transformation [17]:

$$\mathbf{v}_2 = \begin{bmatrix} p \\ q \\ r \end{bmatrix} = \mathbf{J}_2^{-1} \cdot \dot{\mathbf{n}}_2 \tag{7}$$

$$\text{where} \quad \mathbf{J}_2^{-1} = \begin{bmatrix} 1 & 0 & -s\phi_2 \\ 0 & c\phi_1 & c\phi_2 s\phi_1 \\ 0 & -s\phi_1 & c\phi_2 c\phi_1 \end{bmatrix}$$

The yaw rate r (rotation about the l_3 axis) when $\phi_1 = \phi_{\mathbf{nh}1}$ can then be calculated as follows:

$$\begin{aligned} r|_{\phi_1 = \phi_{\mathbf{nh}1}} &= -s\phi_{\mathbf{nh}1} \cdot \omega_2 + c\phi_2 c\phi_{\mathbf{nh}1} \cdot \omega_3 \\ &= -c\phi_{\mathbf{nh}1}\left(t\phi_{\mathbf{nh}1} \cdot \omega_2 - c\phi_2 \cdot \omega_3\right) \end{aligned}$$

According to the above definition (5c), $t\phi_{\mathbf{nh}1} = \frac{c\phi_2 \cdot \omega_3}{\omega_2}$ and consequently $r|_{\phi_1=\phi_{\mathbf{nh}1}} = 0$.

The transformation (7) can also be used to derive the desired body-fixed angular velocities. This is useful in aircraft navigation, as the body-fixed angular velocities are directly actuated.

3.4. Tools from Nonsmooth Analysis

Since the control law (4a) is discontinuous, we will make use of non-smooth analysis tools in the stability proof that follows. Specifically, we will use the extension of Lyapunov theorems to nonsmooth systems that has been presented in [20],[21] and employ Filippov solutions, defined below:

Definition 1. *[22] In the case of a finite dimensional state-space, the vector function $x(.)$ is called a* Filippov solution *of $\dot{x} = f(x)$, where f is measurable and essentially locally bounded, if it is absolutely continuous and $\dot{x} \in K[f](x)$ almost everywhere where $K[f](x) \equiv \overline{co}\{\lim_{x_i \to x} f(x_i) | x_i \notin N_0\}$ and N_0 is a set of measure zero that contains the set of points where f is not differentiable.*

We will use Filippov solutions with the following chain rule to calculate the time derivative of the energy function in the nonsmooth case:

Theorem 1. *[20] Let x be a Filippov solution to $\dot{x} = f(x)$ on an interval containing t and $V : \mathbb{R}^n \to \mathbb{R}$ be a Lipschitz and regular function. Then $V(x(t))$ is absolutely continuous, $(d/dt)V(x(t))$ exists almost everywhere and*

$$\frac{d}{dt}V(x(t)) \in^{a.e.} \dot{\tilde{V}}(x) \triangleq \bigcap_{\xi \in \partial V(x(t))} \xi^T K[f](x(t))$$

where "a.e." stands for "almost everywhere". The notation $\dot{\tilde{V}}(x)$ represents stands for *Clarke's generalized gradient* of V [23]. Finally, we will use the following non-smooth version of LaSalle's invariance principle in the stability proof:

Theorem 2. *[20] Let Ω be a compact set such that every Filippov solution to the autonomous system $\dot{x} = f(x), x(0) = x(t_0)$ starting in Ω is unique and remains in Ω for all $t \geq t_0$. Let $V : \Omega \to R$ be a time independent regular function such that $v \leq 0, \forall v \in \dot{\tilde{V}}$(if $\dot{\tilde{V}}$ is the empty set then this is trivially satisfied). Define $S = \{x \in \Omega | 0 \in \dot{\tilde{V}}\}$. Then every trajectory in Ω converges to the largest invariant set, M, in the closure of S.*

3.5. Stability Analysis

Theorem 3. *The system (1) under the feedback control law (4) is asymptotically stabilised to the destination $\mathbf{n}_{1d}$ with the desired orientation $\mathbf{n}_{2d}$.*

Proof: Since the control law (4) is discontinuous, we will employ Lyapunov analysis for non-smooth systems in the following proof. We will use Φ as a Lyapunov function candidate. The generalized time derivative [20] of Φ is calculated as:

$$\begin{aligned}\dot{\tilde{\Phi}} &= \nabla\Phi^\top \cdot K\left[\dot{\mathbf{n}}\right] = \frac{\partial \Phi}{\partial \mathbf{n}_1}^\top \cdot K[\dot{\mathbf{n}}_1] \\ &\overset{(2)}{=} \frac{\partial \Phi}{\partial \mathbf{n}_1}^\top \cdot \mathbf{J}_I \, K[u]\end{aligned}$$

By (4) we derive for the Filippov set $K[u]$:

$$K[u] = K\left[-\operatorname{sgn}(\mathbf{J}_I^\top \frac{\partial \Phi}{\partial \mathbf{n}_1})\right] \cdot F(\mathbf{n}_1) \tag{8}$$

Finally the generalized time derivative of Φ can be calculated:

$$\begin{aligned}\dot{\tilde{\Phi}} &= \frac{\partial \Phi}{\partial \mathbf{n}_1}^\top \cdot \mathbf{J}_I \cdot K\left[-\operatorname{sgn}\left(\mathbf{J}_I^\top \frac{\partial \Phi}{\partial \mathbf{n}_1}\right)\right] \cdot F(\mathbf{n}_1) \\ &= -\left|\frac{\partial \Phi}{\partial \mathbf{n}_1}^\top \cdot \mathbf{J}_I\right| \cdot F(\mathbf{n}_1) \leq 0\end{aligned}$$

By the non-smooth version of LaSalle's invariance principle [20] we deduce that the system converges to the largest invariant subset included in the set $S \triangleq \left\{\mathbf{n} \,|\, 0 \in \dot{\tilde{\Phi}}\right\}$. Within S, we have

$$0 \in \dot{\tilde{\Phi}} \Longleftrightarrow \mathbf{J}_I^\top \frac{\partial \Phi}{\partial \mathbf{n}_1} \cdot F = 0 \Longleftrightarrow \begin{cases} \mathbf{J}_I^\top \dfrac{\partial \Phi}{\partial \mathbf{n}_1} = 0 & \text{(9a)} \\ \text{or} & \\ F = 0 & \text{(9b)} \end{cases}$$

Conditions (9a) and (9b) define two intersecting sets:

$$S_1 \triangleq \{\mathbf{n} \,|F = 0\} \text{ and } S_2 \triangleq \left\{\mathbf{n} \,\middle|\, \mathbf{J}_I^\top \frac{\partial \Phi}{\partial \mathbf{n}_1} = 0\right\}$$

with $S_1 \bigcup S_2 = S$. The set S_1 includes the points where $\left|\left|\frac{\partial \Phi}{\partial \mathbf{n}_1}\right|\right| = 0$ i.e. the gradient of the potential field is zero, and the current position is the destination i.e. $\mathbf{n}_1 = \mathbf{n}_{1d}$, while for configurations within S_2 the gradient vector is normal to the aircraft's longtitudal axis: $\nabla\Phi \perp l_1$. Since the gradient of the Navigation Function is zero at the destination, it is obvious that the set S_1 consists of the destination with all possible orientations. Since by (6) we have

$$\phi_{\mathbf{nh}k}\big|_{\mathbf{n}_1 = \mathbf{n}_{1d}} = \phi_{kd}, \quad k = 1, 2, 3\,, \tag{10}$$

we define the subset

$$S_3 \triangleq S_1 \bigcap \{\mathbf{n} | \phi_k = \phi_{kd}, \quad k = 1, 2, 3\} \subset S_1$$

which is the destination with the desired orientation angles. By the control law (4) then we deduce that for each configuration inside S_1, where $\phi_k \neq \phi_{kd}$ for at least one of $k = 1, 2, 3$, the corresponding angular velocity is non-zero, steering the agent towards S_3, where all angular velocities fade. Furthermore, $u = 0$ inside $S_1 \supset S_3$, so S_3 is the only invariant subset of S_1.

For the set $S \backslash S_1 \subset S_2$, where $\mathbf{J}_I^\top \frac{\partial \Phi}{\partial \mathbf{n}_1} = \frac{\partial \Phi}{\partial l_1} = 0$ and $F \neq 0$, the potential field's gradient is non-zero and normal to the aircraft's longtitudal axis l_1. In this case, as it will be proven by contradiction below, at least one of the elevation and azimuth angular velocities (ω_2, ω_3) is non-zero and steers the agent away from this set.

Suppose that $\omega_k = 0$ for $k = 1, 2, 3$ inside the set $S \backslash S_1$, this by (4b) means that

$$\phi_{\mathbf{nh}k} = \phi_k, \quad k = 1, 2, 3 \tag{11}$$

Then by the definition of ϕ_{2d} and ϕ_{3d}, (5b) and (5a), we derive:

$$s\phi_2 = s\phi_{\mathbf{nh}2} = \frac{\mathrm{sgn}(x)\Phi_z}{\sqrt{{\Phi_x}^2 + {\Phi_y}^2 + {\Phi_z}^2}} \qquad s\phi_3 = s\phi_{\mathbf{nh}3} = \frac{\mathrm{sgn}(x)\Phi_y}{\sqrt{{\Phi_x}^2 + {\Phi_y}^2}}$$

$$c\phi_2 = c\phi_{\mathbf{nh}2} = \frac{\sqrt{{\Phi_x}^2 + {\Phi_y}^2}}{\sqrt{{\Phi_x}^2 + {\Phi_y}^2 + {\Phi_z}^2}} \qquad c\phi_3 = c\phi_{\mathbf{nh}3} = \frac{\mathrm{sgn}(x)\Phi_x}{\sqrt{{\Phi_x}^2 + {\Phi_y}^2}}$$

when $\sqrt{{\Phi_x}^2 + {\Phi_y}^2} \neq 0$ so that $s\phi_3$, $c\phi_3$ can be calculated as above. Since Navigation Function Φ is polar with exactly one minimum of zero value at the destination, $F \neq 0$ means that at least one of $\left|\left|\frac{\partial \Phi}{\partial \mathbf{n}_1}\right|\right|^2$ and $||\mathbf{n}_1||^2$ is not zero. Taking into account that practically saddle points cannot be reached, the gradient can only be zero at the destination. Therefore outside S_1 we have $\left|\left|\frac{\partial \Phi}{\partial \mathbf{n}_1}\right|\right|^2 \neq 0$ and $||\mathbf{n}_1||^2 \neq 0$, i.e. the navigation function and its gradient are non-zero. Consequently $s\phi_2$, $c\phi_2$ can be calculated in the above way. Substituting for $\mathbf{J}_I$ in (9a) we get: $\mathrm{sgn}(x)\left[{\Phi_x}^2 + {\Phi_y}^2 + {\Phi_z}^2\right] = \mathrm{sgn}(x)\left|\left|\frac{\partial \Phi}{\partial \mathbf{n}_1}\right|\right|^2 = 0$ which is not possible outside S_1. Thus it has been shown that when $\sqrt{{\Phi_x}^2 + {\Phi_y}^2} \neq 0$ inside the set $S \backslash S_1$, the condition (11) cannot hold and consequently by (4b) at least one of ω_2, ω_3 is non-zero.

In the trivial case where inside $S \backslash S_1$, we have $\sqrt{{\Phi_x}^2 + {\Phi_y}^2} = 0 \Leftrightarrow \Phi_x = \Phi_y = 0$, i.e. the gradient lies on the z axis with $\Phi_z \neq 0$ and $s\phi_2 \neq 0$, (9a) yields $\mathrm{sgn}(x) s\phi_2 \Phi_z = 0$ which cannot hold, proving again that (11) is not true in this case either.

We have showed then that in the set $S \backslash S_1$ at least one of the angular velocities ω_2, ω_3 is non-zero, and the set is not invariant. This proves that the only invariant set in S, where every trajectory of the system converges under the proposed control law, is S_3, i.e. the destination $\mathbf{n}_{1d}$ with the desired orientation $\mathbf{n}_{2d}$. Therefore the agent is guaranteed to reach the target, while following an integral line of the potential field, ensuring that the desired orientation will be reached too and no collision will occur. ■

4. INDEPENDENT 3D NAVIGATION WITH COLLISION AVOIDANCE

4.1. Problem Statement

The control scheme presented in the previous section addresses problems involving a single mobile agent. The problem under consideration in this section is to design a control law for each of N spherical agents of radii r_i and state $\mathbf{n}_i$, described by the kinematic model (2). The control scheme must steer each agent i via the inputs: $u_i, \omega_{i1}, \omega_{i2}, \omega_{i3}$ to its desired position and direction (elevation and azimuth angles), $\mathbf{n}_{i1d}$ and ϕ_{i2d}, ϕ_{i3d} respectively, while avoiding collisions with each other or the boundary ∂W of the given workspace $W \subset \mathbb{R}^3$. Each agent is assumed to have knowledge of the position, orientation and longitudinal velocity of all other agents, but not of their destinations. As in the previous section, the workspace is assumed to be spherical of radius r_{world}.

The scenario described above resembles the case of Air Traffic Management (ATM), where each aircraft can monitor the position, orientation and velocity of neighboring aircraft through surveillance. Another possibility is the use of some information exchange system, like *SWIM* (System Wide Information Management) [24], which is envisioned for future design. In any case, each agent needs no knowledge of the destinations other than its own. As the vision for future ATM is towards decentralisation, it is reasonable to expect that each individual aircraft will be able to acquire and process onboard a much increased amount of information. This will be also assisted by technological advances in computing and information systems.

The fact that the method is fully 3D means that each aircraft can use vertical as well as horizontal maneuvering to exploit the available airspace and stay away from conflicts. As the decentralization of Air Traffic Control is thought to be a solution to the increasing air traffic, the control scheme that follows can be useful in the design of future ATM systems. Another application where such an algorithm may be considered is the case of multiple Autonomous Underwater Vehicles (AUVs) operating in the same area.

4.2. Decentralized Dipolar Navigation Functions

In the multi-agent case we use the following Navigation Function:

$$\Phi_i = \frac{\gamma_{di} + f_i}{\left((\gamma_{di} + f_i)^k + H_{nh_i} \cdot G_i \cdot \beta_{0_i}\right)^{1/k}} \tag{12}$$

which is constructed as explained in detail in [25], with the difference that all the vector norms involved are here calculated in the 3D space. The main difference from the Navigation Function for a single agent defined in (3) is the addition of the cooperation term $f_i = f_i(G_i)$. This term is necessary in a decentralized approach, as it is used in proximity situations in order to ensure that Φ_i attains positive values even when agent i has reached its destination. Thus agent i can be temporarily driven away from its destination in order to facilitate the convergence of neighboring agents. Furthermore the function G_i in this case represents a measure of all possible collisions involving agent i: G_i is zero when the i^{th} agent participates in a conflict i.e., when the boundary of the sphere occupied by agent i touches with the boundary of other agents' spheres, and takes positive values away from any conflicts. The reader is referred to [25] for more details on the construction of G_i, f_i. The potential function given above has been used in [9] and has proven navigation properties, i.e., it provides almost global convergence to the destination along with guaranteed collision avoidance.

4.3. Control Law

The proposed control law for the agent i, $i = 1, \ldots, N$ is as follows:

$$u_i = -\, sgn(P_i) \cdot F_i - \left(\frac{\partial \Phi_i}{\partial t} + \left| \frac{\partial \Phi_i}{\partial t} \right| \right) \frac{1}{2P_i} \tag{13a}$$

$$\omega_{i1} = -\, k_{\phi_1} \left(\phi_{i1} - \phi_{\mathbf{nh}i1} \right) \tag{13b}$$

$$\omega_{ik} = -\, k_{\phi_k} \left(\phi_{ik} - \phi_{\mathbf{nh}ik} \right) + \dot{\phi}_{\mathbf{nh}ik}, \quad k = 2, 3 \tag{13c}$$

where

$$\begin{aligned}
F_i =& k_u \cdot ||\nabla_i \Phi_i||^2 + k_z \cdot ||\mathbf{n}_{i1} - \mathbf{n}_{i1d}||^2 \text{ similarly to the single agent case} \\
P_i =& \mathbf{J}_{Ii}^\top \cdot \nabla_i \Phi_i \text{ the projection of gradient } \nabla_i \Phi_i \text{ on agent's } i \text{ longitudal axis } l_{i1} \\
\nabla_i \Phi_j =& \frac{\partial \Phi_j}{\partial \mathbf{n}_{i1}} \text{ the derivative of potential } \Phi_j \text{ wrt agent's } i \text{ position } \mathbf{n}_{i1} \\
\frac{\partial \Phi_i}{\partial t} =& \sum_{j \neq i} u_j \nabla_j \Phi_i^\top \cdot \mathbf{J}_{Ij} \text{ the time derivative of } \Phi_i, \text{ summing the effect of other agents}
\end{aligned}$$

with $\Phi_i = \Phi_i(n_{i1})$ being the above *Dipolar Navigation Function* (12), and k_u, k_z, k_{ϕ_k} positive real gains. The angles $\phi_{\mathbf{nh}ik}$ are defined similarly to the single agent case:

$$\phi_{\mathbf{nh}i3} \triangleq atan2\left(\text{sgn}(p_i)\Phi_{iy}, \text{sgn}(p_i)\Phi_{ix}\right) \tag{14a}$$

$$\phi_{\mathbf{nh}i2} \triangleq atan2\left(\text{-}\,\text{sgn}(p_i)\Phi_{iz}, \sqrt{\Phi_{ix}^2 + \Phi_{iy}^2}\right) \tag{14b}$$

$$\phi_{\mathbf{nh}i1} \triangleq atan2\left(\text{sgn}(p_i)\, c\phi_2 \cdot \omega_3, sgn(p_i)\, \omega_2\right) \tag{14c}$$

where $\Phi_{ix} = \frac{\partial \Phi_i}{\partial x_i}$, $\Phi_{iy} = \frac{\partial \Phi_i}{\partial y_i}$, $\Phi_{iz} = \frac{\partial \Phi_i}{\partial z_i}$, and $p_i = \mathbf{J}_{Iid}^\top \cdot n_{i1}$ is the current position vector with respect to the destination, projected on the longitudinal axis of the desired orientation (l_{i1d}), i.e. $sgn(p_i)$ is equal to 1 in front of the target configuration and -1 behind it. As in the single agent case, $\phi_{\mathbf{nh}i2}$ and $\phi_{\mathbf{nh}i3}$ represent the direction of $\text{sgn}(p_i)\nabla_i \Phi_i$, while $\phi_{\mathbf{nh}i1}$ minimizes the yaw rate of agent i. In order to ensure continuity of the above angles on the destination of agent i, $\mathbf{n}_{i1d}$ (where the gradient vector $\nabla_i \Phi_i$ is zero) we use again the approximation scheme (6), adapted to the multi-agent case :

$$\hat{\phi}_{\mathbf{nh}ik} \triangleq \begin{cases} \phi_{\mathbf{nh}ik}, & \rho_{ik} > \epsilon \\ \dfrac{\phi_{\mathbf{nh}ik}\left(-2\rho_{ik}^3 + 3\epsilon\rho_{ik}^2\right) + \phi_{ikd}\left(-2\left(\epsilon - \rho_{ik}\right)^3 + 3\epsilon\left(\epsilon - \rho_{ik}\right)^2\right)}{\epsilon^3}, & \rho_{ik} \leq \epsilon \end{cases} \tag{15}$$

for $k = 1, 2, 3$, where $\rho_{i1} = \sqrt{c\phi_{i2}^2 \cdot \omega_{i3}^2 + \omega_{i2}^2}$, $\rho_{i2} = ||\nabla_i \Phi_i||$ and $\rho_{i3} = \sqrt{\Phi_{ix}^2 + \Phi_{iy}^2}$. Thus the angles $\hat{\phi}_{\mathbf{nh}ik}$ are continuous at $\rho_{ik} = 0$ as $\lim_{\rho_{ik} \to 0} \hat{\phi}_{\mathbf{nh}ik} = \hat{\phi}_{\mathbf{nh}ik}\Big|_{\rho_{ik}=0} = \phi_{ikd}, k = 1, 2, 3$. Consequently whenever $\mathbf{n}_{i1} = \mathbf{n}_{i1d}$, i.e., agent i is at its target position, we have:

$$\hat{\phi}_{\mathbf{nh}ik} = \phi_{ikd},\ k = 1, 2, 3 \tag{16}$$

As can be seen in the control law for the longitudinal velocity (13a), the term $-\left(\frac{\partial \Phi_i}{\partial t} + \left|\frac{\partial \Phi_i}{\partial t}\right|\right)\frac{1}{2P_i}$ is zero whenever the partial derivative $\frac{\partial \Phi_i}{\partial t}$ is non-positive, while the term is activated when $\frac{\partial \Phi_i}{\partial t} > 0$. As $\frac{\partial \Phi_i}{\partial t}$ sums the effect of all but the i^{th} agent on Φ_i, condition $\frac{\partial \Phi_i}{\partial t} > 0$ implies that the motion of all other agents agents increase Φ_i, and therefore agent i must take that into account to cancel the increasing rate and ensure that its Navigation Function decreases over time. On the contrary, when $\frac{\partial \Phi_i}{\partial t} \leq 0$ the term $-\frac{1}{2P_i}$ is not required and is not used. This modification of the control law results in the term $-\frac{1}{2P_i}$ being used only when absolutely necessary, making the control law less conservative compared to [9], that employs a similar term, as well as more intuitive. The importance of the above will be made clear in the next subsection where the stability analysis is presented.

4.4. Stability Analysis

Theorem 4. *Each agent i described by model (2) under the control law (13) is asymptotically stabilised to its target $\mathbf{n}_{i1d}, \quad \phi_{i2d}, \quad \phi_{i3d}$.*

Proof: We will use again Lyapunov analysis for nonsmooth systems to prove the stability of the system under the control law (13). The following Lyapunov function candidate is used:

$$V = \sum_i V_i, \quad V_i = \Phi_i + \frac{1}{2}\sum_{k=2}^{3} \left(\phi_i - \phi_{\mathbf{nh}ik}\right)^2 \tag{17}$$

The generalized derivative of V [23] is:

$$\partial V = \begin{bmatrix} \sum_i \nabla_1 \Phi_i \\ \vdots \\ \sum_i \nabla_N \Phi_i \\ {}^1\!/_2 \nabla_{\phi_{12}} \left(\phi_{12} - \phi_{\mathbf{nh}12}\right)^2 \\ {}^1\!/_2 \nabla_{\phi_{13}} \left(\phi_{13} - \phi_{\mathbf{nh}13}\right)^2 \\ \vdots \\ {}^1\!/_2 \nabla_{\phi_{N2}} \left(\phi_{N2} - \phi_{\mathbf{nh}N2}\right)^2 \\ {}^1\!/_2 \nabla_{\phi_{N3}} \left(\phi_{N3} - \phi_{\mathbf{nh}N3}\right)^2 \\ {}^1\!/_2 \nabla_{\phi_{\mathbf{nh}12}} \left(\phi_{12} - \phi_{\mathbf{nh}12}\right)^2 \\ {}^1\!/_2 \nabla_{\phi_{\mathbf{nh}13}} \left(\phi_{13} - \phi_{\mathbf{nh}13}\right)^2 \\ \vdots \\ {}^1\!/_2 \nabla_{\phi_{\mathbf{nh}N2}} \left(\phi_{N2} - \phi_{\mathbf{nh}N2}\right)^2 \\ {}^1\!/_2 \nabla_{\phi_{\mathbf{nh}N3}} \left(\phi_{N3} - \phi_{\mathbf{nh}N3}\right)^2 \end{bmatrix} = \begin{bmatrix} \sum_i \nabla_1 \Phi_i \\ \vdots \\ \sum_i \nabla_N \Phi_i \\ \left(\phi_{12} - \phi_{\mathbf{nh}12}\right) \\ \left(\phi_{13} - \phi_{\mathbf{nh}13}\right) \\ \vdots \\ \left(\phi_{N2} - \phi_{\mathbf{nh}N2}\right) \\ \left(\phi_{N3} - \phi_{\mathbf{nh}N3}\right) \\ -\left(\phi_{12} - \phi_{\mathbf{nh}12}\right) \\ -\left(\phi_{13} - \phi_{\mathbf{nh}13}\right) \\ \vdots \\ -\left(\phi_{N2} - \phi_{\mathbf{nh}N2}\right) \\ -\left(\phi_{N3} - \phi_{\mathbf{nh}N3}\right) \end{bmatrix}$$

Let us then consider the multi-agent system $\dot{\mathbf{x}} = f(\mathbf{x})$ resulting from the composition of (2), and its Filippov set [22] $K[f]$:

$$\mathbf{x} = \begin{bmatrix} \mathbf{n}_{11} \\ \vdots \\ \mathbf{n}_{N1} \\ \phi_{12} \\ \phi_{13} \\ \vdots \\ \phi_{N2} \\ \phi_{N3} \\ \phi_{\mathbf{nh}12} \\ \phi_{\mathbf{nh}13} \\ \vdots \\ \phi_{\mathbf{nh}N2} \\ \phi_{\mathbf{nh}N3} \end{bmatrix}, \quad f(\mathbf{x}) = \begin{bmatrix} u_1 \mathbf{J}_{I1} \\ \vdots \\ u_N \mathbf{J}_{IN} \\ \omega_{12} \\ \omega_{13} \\ \vdots \\ \omega_{N2} \\ \omega_{N3} \\ \dot{\phi}_{\mathbf{nh}12} \\ \dot{\phi}_{\mathbf{nh}13} \\ \vdots \\ \dot{\phi}_{\mathbf{nh}N2} \\ \dot{\phi}_{\mathbf{nh}N3} \end{bmatrix}, \quad K[f] = \begin{bmatrix} K[u_1] \mathbf{J}_{I1} \\ \vdots \\ K[u_N] \mathbf{J}_{IN} \\ \omega_{12} \\ \omega_{13} \\ \vdots \\ \omega_{N2} \\ \omega_{N3} \\ \dot{\phi}_{\mathbf{nh}12} \\ \dot{\phi}_{\mathbf{nh}13} \\ \vdots \\ \dot{\phi}_{\mathbf{nh}N2} \\ \dot{\phi}_{\mathbf{nh}N3} \end{bmatrix}$$

By the control law (13a) we deduce:

$$K[u_i] = K[-sgn(P_i)] \cdot F_i - \left(\frac{\partial \Phi_i}{\partial t} + \left| \frac{\partial \Phi_i}{\partial t} \right| \right) \frac{1}{2P_i} \tag{18}$$

Using the chain rule given in [20] we can calculate the generalized time derivative of V as follows:

$$\dot{\tilde{V}} = \bigcap_{\xi \in \partial V} \xi^\top K[f] =$$

$$= \sum_i \sum_j K[u_i] \nabla_i \Phi_j^\top \mathbf{J}_{Ii} + \sum_i \sum_{k=2}^{3} \left(\phi_{ik} - \phi_{\mathbf{nh}ik} \right) \left(\omega_{ik} - \dot{\phi}_{\mathbf{nh}ik} \right) =$$

$$\overset{(18)}{=} \sum_i K[u_i] \nabla_i \Phi_i^\top \mathbf{J}_{Ii} + \sum_i \sum_{j \neq i} K[u_j] \nabla_j \Phi_i^\top \mathbf{J}_{Ij} - \sum_i \sum_{k=2}^{3} k_{\phi_{ik}} \left(\phi_{ik} - \phi_{\mathbf{nh}ik} \right)^2 =$$

$$= \sum_i \left\{ K[-sgn(P_i)] \cdot P_i F_i - \frac{1}{2} \left(\frac{\partial \Phi_i}{\partial t} + \left| \frac{\partial \Phi_i}{\partial t} \right| \right) \right\} + \sum_i \frac{\partial \Phi_i}{\partial t} - \sum_i \sum_{k=2}^{3} k_{\phi_k} \left(\phi_{ik} - \phi_{\mathbf{nh}ik} \right)^2 =$$

$$= \sum_i \left\{ - \left| P_i \right| F_i - \frac{1}{2} \left(\left| \frac{\partial \Phi_i}{\partial t} \right| - \frac{\partial \Phi_i}{\partial t} \right) \right\} - \sum_i \sum_{k=2}^{3} k_{\phi_k} \left(\phi_{ik} - \phi_{\mathbf{nh}ik} \right)^2 \leq 0$$

Since each V_i and consequently V is regular [23] and the level sets of V are compact, the nonsmooth version of LaSalle's invariance principle [20] can be applied. We can thus conclude that all the trajectories of the closed-loop system converge to the largest invariant subset S:

$$S \triangleq \left\{ \mathbf{n} \,|\, 0 \in \dot{\tilde{V}} \right\} = \left\{ \mathbf{n} : \forall i, \left(- \left| P_i \right| F_i - \frac{1}{2} \left(\left| \frac{\partial \Phi_i}{\partial t} \right| - \frac{\partial \Phi_i}{\partial t} \right) = 0 \right) \wedge \left(\phi_{ik} = \phi_{\mathbf{nh}ik}, k = 2, 3 \right) \right\}$$

Thus inside S we have $P_i = 0$ or $F_i = 0$ for each agent i The condition $F_i = 0$ holds only when $\mathbf{n}_{i1} = \mathbf{n}_{i1d}$, i.e., when agent i has reached its target position, while P_i holds at the target and whenever the agent's i longitudinal axis is normal to the field's gradient $\nabla_i \Phi_i$. In the latter case though, at least one of the elevation and azimuth angles ϕ_{i2} and ϕ_{i3} are not equal with $\phi_{\mathbf{nh}i2}$ and $\phi_{\mathbf{nh}i3}$ respectively, and therefore the corresponding configurations are outside S. As a result, only the target positions $\mathbf{n}_{i1} = \mathbf{n}_{i1d} \forall i$ is included in S. Moreover, by (16) and the condition $\phi_{ik} = \phi_{\mathbf{nh}ik} \forall i, k = 2, 3$, we deduce that the set S reduces to the singleton $\{\mathbf{n} : \forall i, (\mathbf{n}_{i1} = \mathbf{n}_{i1d}) \wedge (\phi_{ik} = \phi_{ikd}, k = 2, 3)\}$, i.e., all the agents are stabilised to their destinations with the desired elevation and azimuth angles. ■

Remark: From the control law (13a) we can see that the linear velocity can tend to infinite values when $P_i \to 0$, i.e., when the projection of the field's gradient on the agent's longitudinal axis becomes very small. This is the case when the gradient vector is normal to the agent's longitudinal axis l_{i1}: $\nabla_i \Phi_i \perp l_{i1}$. As mentioned above, in this case at least one of the angles ϕ_{ik}, $k = 2, 3$ will not be equal to the the corresponding $\phi_{\mathbf{nh}ik}$, and therefore $(\phi_{ik} - \phi_{\mathbf{nh}ik})$ is non-zero for at least one of $k = 2, 3$. Calculating the dynamics of this term we have:

$$\frac{d}{dt}(\phi_{ik} - \phi_{\mathbf{nh}ik}) = -k_{\phi_k}(\phi_i k - \phi_{\mathbf{nh}ik}) + \dot{\phi}_{\mathbf{nh}ik} - \dot{\phi}_{\mathbf{nh}ik}$$

As a result the absolute value $|\phi_{ik} - \phi_{\mathbf{nh}ik}|$ is always decreasing in time and each term $\phi_{ik} - \phi_{\mathbf{nh}ik}$, $k = 2, 3$ is stabilised to 0. Therefore if the absolute angle between the field's gradient and l_{i1} is initaly

smaller than $\frac{\pi}{2}$, it will always remain in $\left[0, \frac{\pi}{2}\right)$. Thus the set $G \triangleq \{\mathbf{n} \,|\, \exists i : \nabla_i \Phi_i \perp l_{i1}\}$, where $P_i \to 0$, will never be reached. Essentially, what is required is

$$P_i \cdot p_i > 0$$

at the initial conditions, i.e. agents starting in the subspace behind their targets (where $p_i < 0$) must have the initial negated gradient vector driving them forward ($P_i < 0$), while agents starting in front of their target ($p_i > 0$) must have the negated gradient initially driving them backward ($P_i > 0$). To enforce additionally only forward (or backward) motion, preventing any direction reversals, all agents must start in the subspace behind (or in front) of their targets. These mild requirements should not pose practical difficulties in Air Traffic applications, since they represent reasonable physical conditions.

5. Simulations

5.1. Single Agent Scenario

The control strategy presented in Section 3 has been used on a computer simulation. The test case consisted of a workspace with $r_{world} = 150$, containing 3 obstacles of various radii scattered in the workspace . The initial configuration of the agent has been set at

$$\mathbf{n}_{init} = \left[\begin{array}{cccccc} -90 & 90 & 30 & 0 & \frac{\pi}{4} & -\frac{3\pi}{2} \end{array} \right]^\top$$

The goal is to drive the agent to the origin with zero azimuth, elevation and bank angles, i.e. $\mathbf{n}_{1d} = \left[\begin{array}{ccc} 0 & 0 & 0 \end{array} \right]^\top$, $\mathbf{n}_{2d} = \left[\begin{array}{ccc} 0 & 0 & 0 \end{array} \right]^\top$. The resulting trajectory of the agent is presented in Figures 4(a) and 4(b) from different viewing angles. The agent follows a feasible, nonholonomic 3-dimensional path avoiding all the obstacles, and converges to the target with the desired orientation. Furthermore, it can be seen that the bank angle control law rotates the agent so that the body-fixed yaw rotation rate is maintained low, as intended. The efficiency of this is specifically demonstrated in Figure 5, where the resulting yaw rotation rate is presented, in comparison with the 3 earth-fixed rotation rates.

5.2. Multi-agent Scenario

The test case considered here consists of 4 agents of radii $r_i = 0.05$, $i = 1, \ldots, 4$ operating in a spherical workspace of $r_{world} = 1$. The initial positions are spanned near the boundary of the workspace facing inward and the target configurations have been set across the center of the workspace, so that the straight line paths between each start position and the corresponding destination converge in the center. Specifically the initial configurations of the agents are:

$$\begin{aligned}
\mathbf{n}_{1init} &= \left[\begin{array}{cccccc} -0.9 & 0 & 0.3 & 0 & 0 & 0 \end{array} \right]^\top \\
\mathbf{n}_{2init} &= \left[\begin{array}{cccccc} 0 & -0.9 & -0.4 & 0 & 0 & \frac{\pi}{2} \end{array} \right]^\top \\
\mathbf{n}_{3init} &= \left[\begin{array}{cccccc} 0.6 & 0.6 & -0.4 & 0 & 0 & -\frac{3\pi}{4} \end{array} \right]^\top \\
\mathbf{n}_{4init} &= \left[\begin{array}{cccccc} 0.6 & -0.6 & -0.2 & 0 & 0 & \frac{3\pi}{4} \end{array} \right]^\top
\end{aligned}$$

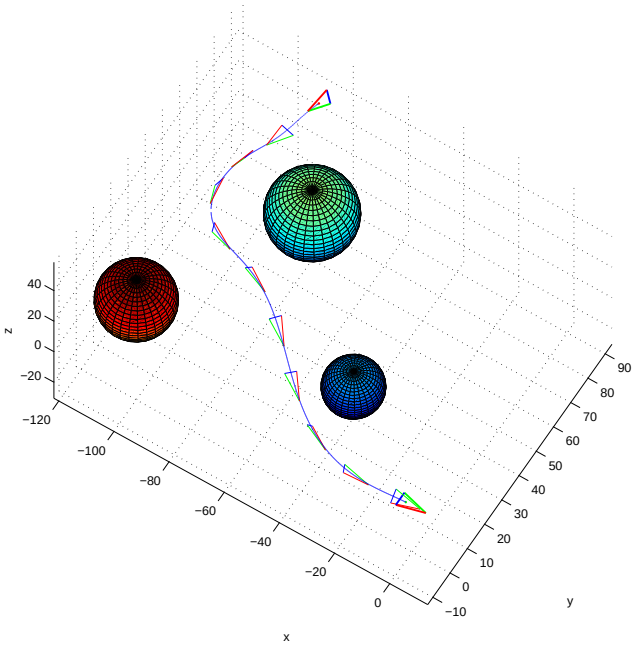

(a)

Figure 4: Agent's Path in 3D Space

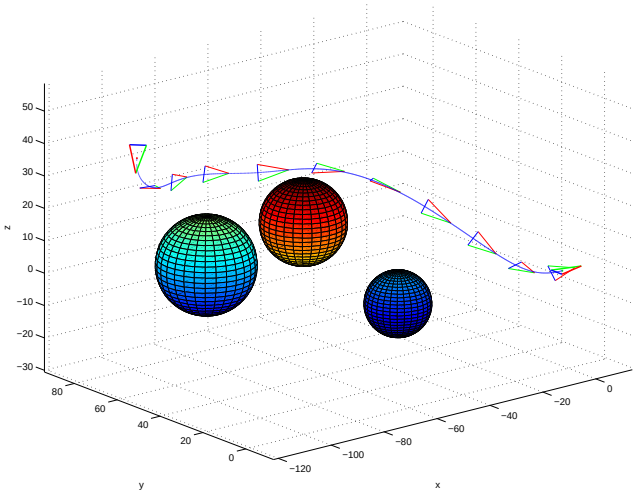

(b)

Figure 4: Agent's Path in 3D Space (cont.)

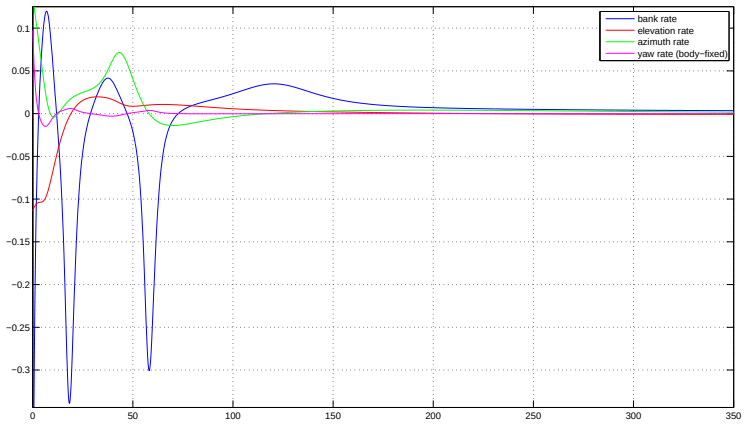

Figure 5: Rotation rates history

and the target positions and elevation, azimuth angles :

$$\begin{aligned}
\mathbf{n}_{11d} &= [\ 0.9 \quad 0 \quad -0.3]^\top, \quad \phi_{12d} = 0, \quad \phi_{13d} = 0 \\
\mathbf{n}_{21d} &= [\ 0 \quad 0.9 \quad 0.2]^\top, \quad \phi_{22d} = 0, \quad \phi_{23d} = \tfrac{\pi}{2} \\
\mathbf{n}_{31d} &= [-0.6 \quad -0.6 \quad 0.2]^\top, \quad \phi_{32d} = 0, \quad \phi_{33d} = -\tfrac{3\pi}{4} \\
\mathbf{n}_{41d} &= [-0.6 \quad 0.6 \quad 0.4]^\top, \quad \phi_{42d} = 0, \quad \phi_{43d} = \tfrac{3\pi}{4}
\end{aligned}$$

The trajectories of the agents are plotted in Figures 6(a), 6(b) and 6(c). The distances between any two agents are plotted in Figure 7 (solid lines), along with the minimum safety clearance, which is double the radius of each agent $2 \cdot r_i = 0.1$. All agents follow feasible, nonholonomic 3-dimensional paths avoiding collisions with each other, and converge to their destinations and directions as intended. The distance between any two agents remains always greater than the safety margin as no collisions occur.

6. Conclusions

This paper proposes a Navigation Function based control strategy for single and multiple 3-dimensional nonholonomic aircraft-like agents. In the single agent case the agent is driven to its target, while avoiding all obstacles and the workspace's boundary. In the multi-agent case the distributed control scheme steers the agents towards their targets and away from collisions with each other. In both cases the resulting trajectories respect the nonholonomic constraints and the low yaw capability of typical aircraft. The use of a feedback law offers fast response and makes the control strategy robust with respect to measurement and modeling errors, while Navigation Functions provide guaranteed global convergence and collision avoidance.

Future work in this area focuses on the incorporation of input constraints, so that the algorithm complies with aircraft's performance characteristics. One possible way of achieving this may come from using the notion of reserved region [26]. Other research directions include the incorporation of a limited sensing scheme, like the one used in [27] or [28]. This will further decentralise our algorithm, and will significantly reduce the amount of required information in a real ATM scenario.

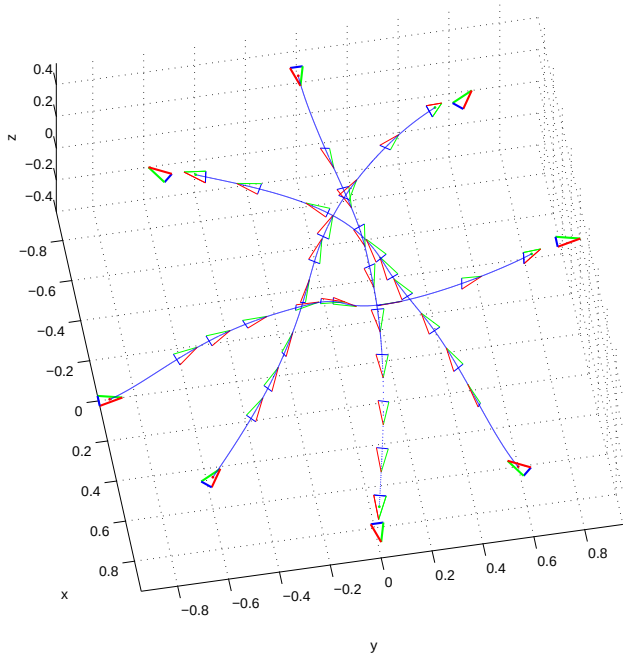

(a)

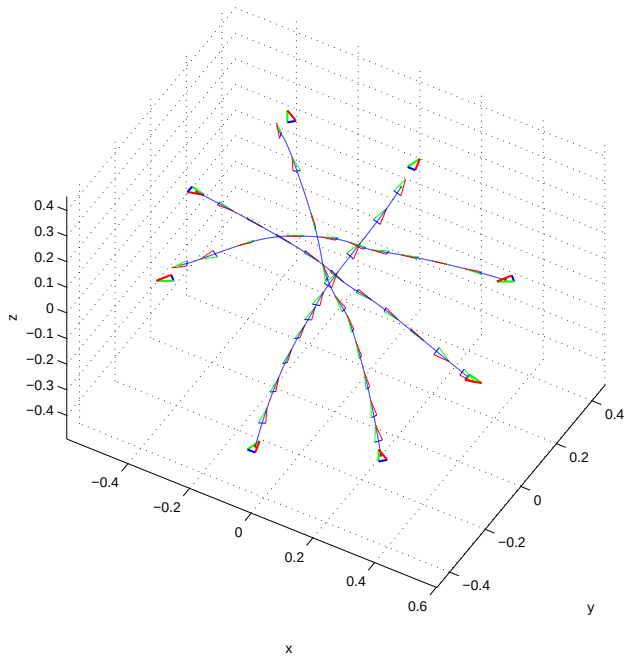

(b)

Figure 6: 4 Agents Navigating in 3D Space

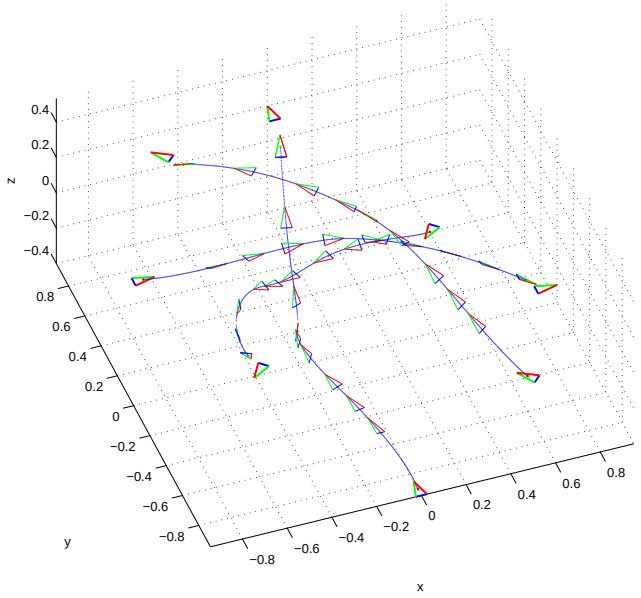

(c)

Figure 6: 4 Agents Navigating in 3D Space (cont.)

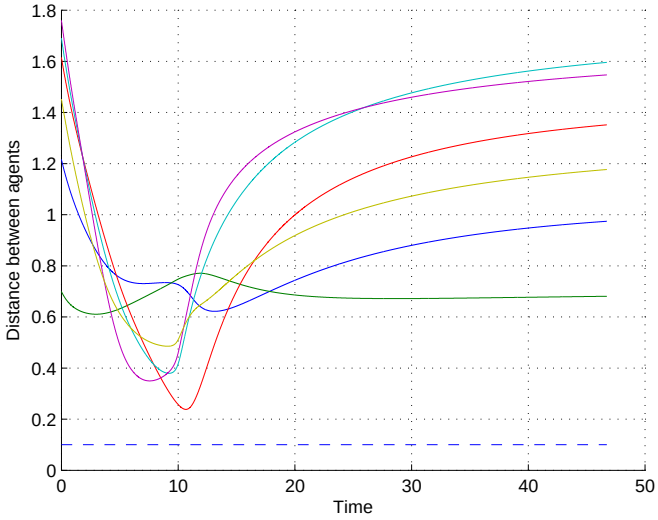

Figure 7: Distances between agents (solid lines) and minimum safety clearance (dashed line)

ACKNOWLEDGEMENT

Giannis Roussos and Kostas J. Kyriakopoulos want to acknowledge the contribution of the European Commission through project iFLY. Dimos Dimarogonas is partially supported by the NASA IDEAS project.

REFERENCES

1. Bloch AM. *Nonholonomic Mechanics and Control*. Springer-Verlag NY, 2003.
2. Brockett RW. Asymptotic stability and feedback stabilization. *Differential Geometrics in Control Theory, Progress in Mathematics,* vol. 27, Robert W Brockett RSM, Sussmann HJ (eds.). Birkhauser Publishers: Boston, 1983; 181–191.
3. Astolfi A. Exponential stabilization of a wheeled mobile robot via discontinuous control. *ASME Journal of Dynamic Systems Measurement and Control* 1999; **121**:121–125.
4. Canudas-de-Wit C, Sordalen OJ. Exponential stabilization of mobile robots with nonholonomics constraints. *IEEE Transaction on Automatic Control* 1992; **37**(11).
5. Bloch AM, Drakunov SV, Kinyon MK. Stabilization of nonholonomic systems using isospectral flows. *SIAM Journal on Control and Optimization* 2000; **38**(3):855–874.
6. Rimon E, Koditschek DE. Exact robot navigation using artificial potential functions. *IEEE Transactions on Robotics and Automation* 1992; **8**(5):501–508.
7. Lopes GAD, Koditschek DE. Navigation functions for dynamical, nonholonomically constrained mechanical systems. *Advances in Robot Control*, Kawamura S, Svinin M (eds.). Springer, 2006; 135–155.
8. Tanner HG, Loizou S, Kyriakopoulos KJ. Nonholonomic navigation and control of cooperating mobile manipulators. *IEEE Transactions on Robotics and Automation* 2003; **19**(1):53–64.
9. Loizou SG, Dimarogonas DV, Kyriakopoulos KJ. Decentralized feedback stabilization of multiple nonholonomic agents. *Proceedings of the 2004 International Conference on Robotics and Automation*, 2004; 3012–3017.
10. Aicardi M, Cannata G, Casalino G, Indiveri G. Guidance of 3D underwater non-holonomic vehicle via projection on holonomic solutions. *Symposium on Underwater Robotic Technology, SURT 2000*, June 2000.
11. Aicardi M, Casalino G, Indiveri G. Closed loop control of 3D underactuated vehicles via velocity field tracking. *Advanced Intelligent Mechatronics, 2001. Proceedings. 2001 IEEE/ASME International Conference on* 2001; **1**:355–360.
12. Ambrosino G, Ariola M, Ciniglio U, Corraro F, Pironti A, Virgilio M. Algorithms for 3D UAV path generation and tracking. *2006 45th IEEE Conference on Decision and Control*, 2006; 5275–5280.
13. Roussos GP, Dimarogonas DV, Kyriakopoulos KJ. 3D navigation and collision avoidance for a non-holonomic vehicle. *2008 American Control Conference, Seattle, Washington, USA* 2008; :3512–3517.
14. Tomlin CJ, Pappas GJ, Sastry SS. Conflict resolution for air traffic management: A study in multiagent hybrid systems. *IEEE Transactions on Automatic Control* 1998; **43**:509–521.
15. Bicchi A, Pallottino L. On optimal cooperative conflict resolution for air traffic management systems. *IEEE Transactions on Intelligent Transportation Systems* 2000; **1**(4):221–231.
16. Inalhan G, Stipanovic D, Tomlin C. Decentralized optimization, with application to multiple aircraft coordination. *Proceedings of the* 41^{st} *Conference on Decision and Control*, 2002.
17. Fossen TI. *Guidance and Control of Ocean Vehicles*. John Wiley & Sons, 1994.
18. Breivik M, Fossen T. Principles of guidance-based path following in 2D and 3D. *Decision and Control, 2005 and 2005 European Control Conference. CDC-ECC '05. 44th IEEE Conference on*, 2005; 627–634.
19. Egerstedt M, Hu X. Formation constrained multi-agent control. *Robotics and Automation, IEEE Transactions on* Dec 2001; **17**(6):947–951.
20. Shevitz D, Paden B. Lyapunov stability theory of nonsmooth systems. *IEEE Transactions on Automatic Control* 1994; **39**(9):1910–1914.
21. Ceragioli F. Discontinuous ordinary differential equations and stabilization. PhD Thesis, Dept. of Mathematics, Universita di Firenze 2000.
22. Filippov A. *Differential equations with discontinuous right-hand sides*. Kluwer Academic Publishers, 1998.
23. Clarke F. *Optimization and Nonsmooth Analysis*. Addison-Wesley, 1983.
24. Single European Sky ATM Research - SESAR. European ATM Master Plan 2009.
25. Dimarogonas DV, Loizou SG, Kyriakopoulos KJ, Zavlanos MM. A feedback stabilization and collision avoidance scheme for multiple independent non-point agents. *Automatica* 2006; **42**(2):229–243.
26. Pallottino L, Scordio VG, Frazzoli E, Bicchi A. Decentralized cooperative policy for conflict resolution in multi-vehicle systems. *IEEE Trans. on Robotics* 2007; **23**(6):1170–1183.
27. Dimarogonas DV, Kyriakopoulos KJ, Theodorakatos D. Totally distributed motion control of sphere world multi-agent systems using decentralized navigation functions. *Proceedings of the 2006 IEEE International Conference on Robotics & Automation*, 2006; 2430–2435.
28. Keviczky T, Borrelli F, Fregene K, Godbole D, Balas GJ. Decentralized receding horizon control and coordination of autonomous vehicle formations. *Control Systems Technology, IEEE Transactions on* 2008; **16**(1):19–33.